Galectin 1 Proangiogenic and Promigratory Effects in the Hs683 Oligodendroglioma Model Are Partly Mediated through the Control of *BEX2* Expression[1]

Marie Le Mercier*, Shannon Fortin*, Véronique Mathieu*, Isabelle Roland[†], Sabine Spiegl-Kreinecker[‡], Benjamin Haibe-Kains[§,¶], Gianluca Bontempi[¶], Christine Decaestecker*, Walter Berger[#], Florence Lefranc*,** and Robert Kiss*

*Laboratory of Toxicology, Institute of Pharmacy, Université Libre de Bruxelles (ULB), Brussels, Belgium; [†]Department of Pathology, Erasme University Hospital, ULB, Brussels, Belgium; [‡]Department of Neurosurgery, Wagner Jauregg Hospital, Linz, Austria; [§]Functional Unit, Jules Bordet Institute, Brussels, Belgium; [¶]Machine Learning Group, Department of Computer Science, ULB, Brussels, Belgium; [#]Institute of Cancer Research, Department of Medicine I, Medical University of Vienna, Austria; **Department of Neurosurgery, Erasme University Hospital, ULB, Brussels, Belgium

Abstract

We have previously reported that galectin 1 (Gal-1) plays important biological roles in astroglial as well as in oligodendroglial cancer cells. As an oligodendroglioma model, we make use of the Hs683 cell line that has been previously extensively characterized at cell biology, molecular biology, and genetic levels. Galectin 1 has been shown to be involved in Hs683 oligodendroglioma chemoresistance, neoangiogenesis, and migration. Down-regulating Gal-1 expression in Hs683 cells through targeted small interfering RNA provokes a marked decrease in the expression of the brain-expressed X-linked gene: *BEX2*. Accordingly, the potential role of *BEX2* in Hs683 oligodendroglioma cell biology has been investigated. The data presented here reveal that decreasing *BEX2* expression in Hs683 cells increases the survival of Hs683 orthotopic xenograft-bearing mice. Furthermore, this decrease in BEX2 expression impairs vasculogenic mimicry channel formation *in vitro* and angiogenesis *in vivo*, and modulates glioma cell adhesion and invasive features through the modification of several genes previously reported to play a role in cancer cell migration, including *MAP2*, *plexin C1*, *SWAP70*, and *integrin* β_6. We thus conclude that *BEX2* is implicated in oligodendroglioma biology.

Neoplasia (2009) 11, 485–496

Introduction

Gliomas are the most common primary brain malignancy found in adults [1,2]. High-grade gliomas of astrocytic origin are characterized by the diffuse invasion of distant brain tissue by a myriad of single migrating cells with reduced susceptibility to apoptosis and consequent resistance to the cytotoxic insults of proapoptotic drugs [2]. Current recommendations are that patients with high-grade astrogliomas (including glioblastoma multiforme, GBM) should undergo maximum surgical resection, followed by concurrent radiation and chemotherapy with the alkylating drug temozolomide (TMZ) [3]. Oligodendrogliomas are rare and diffusely infiltrating tumors arising

in the white matter of cerebral hemispheres and display better sensitivity to treatment and a better prognosis than other gliomas [4].

Chronic platelet-derived growth factor signaling in glial progenitors leads to the formation of oligodendrogliomas in mice, whereas chronic combined Ras and Akt signaling leads to astrocytomas [5]. The different histologies of these tumors imply that the pathways activated by these two oncogenic stimulations are different and that the apparent lineage of the tumor cells may result from specific signaling activity [5]. Combined activation of Ras and AKT leads to the formation of astrocytic GBM in mice [6]. In human GBMs, AKT is not mutated but is activated in approximately 70% of these tumors, in association with loss of PTEN and/or activation of receptor tyrosine kinases [6]. Oligodendrogliomas with 1p19q codeletion harbor a gene expression profile that partially resembles the gene expression of normal brain samples, whereas gliomas with epidermal growth factor receptor amplification express many genes in common with glioblastoma cancer stem cells [7]. Neuronal differentiation could occur in oligodendrogliomas with 1p19q codeletion and the cell of origin for gliomas with 1p19q codeletion could be a bipotential progenitor cell, able to give rise to both neurons and oligodendrocytes [7].

Galectin 1 (Gal-1) belongs to a family of 15 carbohydrate-binding proteins with affinity for β-galactosides [8,9] and has been shown to play an important role in astroglioma and oligodendroglioma cell biology [9]. For example, Gal-1 is a key player in astroglioma and oligodendroglioma cell migration [10–12]. Galectin 1 expression is increased under hypoxic conditions [13], and radiotherapy stimulates Gal-1 expression in glioma cells [14].

We have recently demonstrated that TMZ stimulates Gal-1 expression in the Hs683 oligodendroglioma model [15] and that decreasing Gal-1 expression in these Hs683 cells increases the antitumor effects contributed by TMZ both *in vitro* and *in vivo* [15,16].

Galectin 1 is a key player in tumor neoangiogenesis [17], and we have recently demonstrated that Gal-1 exerts its proangiogenic effects in human Hs683 oligodendrogliomas through the endoplasmic reticulum transmembrane kinase/ribonuclease inositol-requiring 1α (IRE-1α)–mediated control of the expression of oxygen-related protein 150, which, in turn, controls vascular endothelial growth factor (VEGF) maturation [16].

We observed that down-regulating Gal-1 expression in Hs683 human oligodendroglioma cells through targeted small interfering RNA (siRNA) provokes a marked decrease in the expression of the brain-expressed X-linked gene. *BEX2*, which belongs to a small family of six genes with a wide distribution among tissue types [18,19], is found highly expressed in the embryonic brain [20]. *BEX2* is described as a tumor suppressor gene in astrogliomas [21] and has been implicated in apoptotic features of breast cancer [22]. The role of *BEX2* in oligodendroglioma biology has never been investigated, at least to the best of our knowledge, and therefore represents the aim of the present work. As a human oligodendroglioma model, we made use of the Hs683 cell line, whose oligodendroglial origin has been extensively characterized. Indeed, Hs683 tumor cells are 1p19q codeleted [23] and are highly sensitive to chemotherapy under *in vivo* orthotopic brain xenograft conditions [23]. These cells display very weak (if any) *vimentin* expression and high levels of *integrin β4* expression [24] as do oligodendrogliomas [24,25]. Hs683 cells do not express the human 1p-distal *ATAD 3B* gene, which is highly expressed in astroglioma cells [26]. However, they contain only one *Notch2* gene copy per diploid genome as do oligodendrogliomas [27], in which loss of the 1p centromeric marker within intron 12

of the *Notch2* gene is associated with a favorable prognosis in oligodendroglioma patients [28,29].

Materials and Methods

Cell Cultures and Compounds

The Hs683 (ATCC code HTB-138), U87 (ATCC code HTB-14), U373 (ATCC code HTB-17), and T98G (ATCC code CRL-1690) human glioma cell lines were obtained from the American Type Culture Collection (ATCC, Manassas, VA) and maintained in our laboratory as detailed previously [15,16,23,24].

We also made use of four primocultures established in our facilities as detailed previously [30]. Briefly, glioma tumor specimens were transferred during surgery into culture medium (RPMI-1640 with 20% fetal calf serum [FCS], 1% glutamine, 1% penicillin/streptomycin). The tissue was gently disrupted and washed with physiological saline to remove red blood cells. After passage 5, cells were grown in a culture medium containing 10% FCS without antibiotics. These primocultures have been labeled GL-5, GL-16, GL-17, and GL-19 in the current study. They are part of a collection of several hundred glioma primocultures established in the Department of Neurosurgery of the Wagner Jauregg Hospital (Linz, Austria).

Anti–Gal-1 siRNA and Anti-BEX2 siRNA

The sequence of the siRNA (Eurogentec, Seraing, Belgium) used in the current work are listed below. For Gal-1, the sense sequence was 5′-gcugccagauggauacgaadtdt-3′ and the antisense sequence was 5′-uucguauccaucuggcagcdtdt-3′ [15,16]. For BEX2, the sense sequence was 5′-gcaggagaguuuuaccuaudtdt-3′ and the antisense sequence was 5′-auaggUaaaacucuccugcdtdt-3′. A corresponding nonspecific sequence siRNA (designated throughout as CT siRNA) was used as a process control (sense, 5′-ggaaaucccccaacagugadtdt-3′; antisense, 5′-ucacuguuggggGauuuccdtdt-3′). The antisense and sense strands of the siRNA were annealed by the manufacturer in 50 mM Tris, pH 7.5 to 8.0, and 100 mM NaCl in diethylpyrocarbonate–treated water. The final concentration of siRNA duplexes was 100 μM.

Hs683 glioma cells were either left untreated (wild type: wt) or were transfected with calcium phosphate (Kit ProFection mammalian transfection system; Promega, Leiden, the Netherlands) containing the specified siRNA for 16 hours (day 0). On day 1, the transfection procedure was repeated. On day 2, each group of cells was pooled and replated for subsequent experiments. On days 5, 7, 9, 12, and 14, Hs683 cells were either scraped into cold PBS buffer (for RNA extraction) or lysed directly in boiling lysis buffer (10 mM Tris pH 7.4, 1 mM Na_3VO_4, 1% SDS, pH 7.4) for protein extraction. Hs683 cells were also cultured on glass coverslips for immunofluorescence (IF) analyses as detailed previously [15,16]. The efficiency of the anti–Gal-1 siRNA was evaluated by means of Western blot (WB) analysis and/or IF and the efficiency of the anti-BEX2 siRNA was evaluated by means of IF and/or reverse transcription–polymerase chain reaction (RT-PCR).

In Vitro *Transfection of Anti-BEX2 siRNA into Hs683 Cells and Their Grafting into the Brains of Immunocompromised Mice*

Hs683 glioma cells were transfected *in vitro* with anti-BEX2 siRNA or CT siRNA as detailed above. Hs683 cells were grafted orthotopically into the brains of nude mice as described previously [31]. In each experiment, all mice (8-week-old female *nu/nu* mice, 21-23 g; Iffa

Credo, Charles Rivers, Arbresle, France) had 100,000 Hs683 cells (wt, CT siRNA-transfected, or anti-*BEX2* siRNA-transfected) stereotactically implanted on the same day (day 5 after siRNA transfection). Each experimental group contained 11 mice. All the *in vivo* experiments described in the present study were performed on the basis of Authorization No. LA1230509 of the Animal Ethics Committee of the Federal Department of Health, Nutritional Safety and the Environment (Belgium).

In Vivo *Determination of Tumor Neoangiogenesis*

Each mouse bearing a brain Hs683 glioma underwent euthanasia (in a CO_2 atmosphere) for ethical reasons when it had lost 20% of its body weight compared with that recorded on the day of tumor grafting. The brain was removed from the skull, fixed in buffered formalin for 48 hours, embedded in paraffin, and cut into 5-μm-thick sections.

After heat-induced antigen retrieval in citrate buffer (pH 6.0), sections were exposed to 0.4% hydrogen peroxide for 30 minutes to quench endogenous peroxydase. The sections were then incubated with an anti-CD34 antibody (diluted 1:25; Abcam, Cambridge, United Kingdom) for 1 hour at room temperature. For visualization of antigen location, the Poly-HRP IHC Detection Systems (ImmunoLogics, Duiven, the Netherlands) method and 3,3'-diaminobenzidine (Biogenex, Klinipath, Olen Belgium) were used. Finally, the sections were counterstained with hematoxylin.

The stained blood vessels were counted using a grid as indicated previously [31,32]. Typical blood vessels analyzed are illustrated in Figure 3*B*. Fifteen fields at a G×40 magnification were analyzed per histological slide, giving thus a total of 165 histological fields per group.

In Vitro *Determination of the Capacity of Hs683 Cells to Undergo Vasculogenic Mimicry*

Petri dishes, 35 mm in diameter, were precoated with Matrigel and then incubated at 37°C for 10 minutes. Hs683 wild-type cells, transfected with CT siRNA or transfected with anti-*BEX2* siRNA (400,000 cells per Petri dish) were seeded on the coated Petri dishes at day 5 after transfection and cultivated for 48 hours. The ability of these cells to perform vasculogenic mimicry-like processes was assessed qualitatively at 24 and 48 hours after seeding as described previously [16].

In Vitro *Determination of Anchorage-Dependent Cell Growth*

Anchorage-dependent cell growth was assessed using the 3-[4,5-dimethylthiazol-2yl]-diphenyltetrazolium bromide (MTT; Sigma, Bornem, Belgium) colorimetric assay, as detailed elsewhere [33]. All determinations were carried out in sextuplicate.

In Vitro *Determination of Anchorage-Independent Cell Growth*

Anchorage-independent cell growth was assessed using the soft agar clonogenic assay as previously described [34]. All determinations were carried out in sextuplicate.

In Vitro *Quantitative Determination of Cell Migration*

Cell motility was characterized using computer-assisted phase-contrast microscopy (quantitative videomicroscopy), which enables the trajectories of living cells maintained in culture to be quantified [33,35]. The greatest linear distance migrated by each cell (out of hundreds of cells analyzed per experimental condition) was calculated

from these trajectories [33,35]. All experiments were performed for 72 hours with one image recorded every 4 minutes. All determinations were carried out in triplicate.

In Vitro *Determination of Hs683 Cell-Invasive Features*

Invasive features of Hs683 cells *in vitro* were assessed by means of the Boyden transwell invasion system (BD BioCoat Matrigel invasion chambers; BD Biosciences Discovery Labware, Bedford, MA) as detailed elsewhere [35].

In Vitro *Adhesion Assay*

The adhesion assay was performed as described previously [36] with modifications. Six-well plates were precoated with Matrigel (diluted 1:3 in RPMI culture medium with 10% FCS) or with 10 μg/ml of the 120-kDa fragment of fibronectin (Chemicon, Biognost, Waterven, Belgium) for 1 hour at 37°C. The wells were washed, and nonspecific binding was then blocked with 0.1% BSA in PBS for 30 minutes. Hs683 cells (100,000 cells per well) were allowed to adhere for 1 hour at 37°C, after which nonadherent cells were gently washed away with warm PBS. Adherent cells were formalin-fixed, hematoxylin-stained, and counted in 10 fields per well at a G×10 magnification using an Olympus microscope (Olympus, Antwerp, Belgium).

Determination of BEX1 *and* BEX2 *Genomic Expression in a Clinical Series of 153 Gliomas and 23 Normal Brain Samples*

The genomic expression of *BEX1* and *BEX2* was analyzed in a series of 176 human brain samples, including 23 normal brain tissues, 7 grade 2 astrocytomas, 19 grade 3 astrocytomas, 77 GBMs, 38 grade 2 oligodendrogliomas, and 12 grade 3 oligodendrogliomas. Microarray data were generated by the Henry Ford Hospital (Detroit, MI) from the Affymetrix Array Series GSE4290: http://www.ncbi.nlm.nih.gov/geo/query/acc.cgi?acc=GSE4290.

Genomic and Proteomic Analyses

Genomic analyses   RNA was extracted from wt Hs683 cells or from those transfected with CT siRNA or specific siRNA directed against Gal-1 or *BEX2*, and the quality and integrity of the extracted RNA was assessed as detailed previously [33,35]. Full genome analyses were performed on day 5 of transfection at the VIB Microarray Facility (UZ Gasthuisberg, Catholic University of Leuven, Leuven, Belgium) using the Affymetrix Human Genome U133 set Plus 2.0 (High Wycome, UK). Microarray data analyses were undertaken as detailed previously [15,16,32].

Protein expression measurements   Western blot and IF analyses were performed as detailed previously [16,31–33]. Control experiments included the omission of the incubation step with the primary antibodies (negative control). Equal loading was verified by the bright Ponceau red coloration of the membranes. The integrity and quantity of the extracts were assessed by means of tubulin immunoblot analysis. The following primary antibodies were used for WB analysis: anti–Gal-1 (dilution 1:1000; Preprotech TebuBio, Boechout, Belgium), anti–integrin $β_6$ (dilution 1:100; Calbiochem, VWR International, Leuven, Belgium), anti-plexinC1 (dilution 1:1000; R&D Systems, Abingdon, United Kingdom), anti-VEGF (dilution 1:500; Santa Cruz; TebuBio), anti–switch-associated protein 70 (SWAP70; dilution 1:500; Novus Biologicals; DivBioscience, Breda, the Netherlands), and anti–IRE-1α (dilution 1:500; Cell Signaling, Bioké, Leiden, the

Netherlands). Secondary antibodies were purchased from Pierce (PerbioScience, Erembodegem, Belgium) for the WB s and from Molecular Probes (Invitrogen, Merelbeke, Belgium) for fluorescent detection (Alexa Fluor–conjugated antibodies).

Western blots were developed using the Pierce Supersignal Chemiluminescence system (Pierce, Perbio Science N.V., Aalst, Belgium). The staining patterns were also assessed by immunofluorescence for *BEX2* (dilution 1:50; Abcam) and integrin β_6 (dilution 1:50) and were analyzed by means of a computer-assisted fluorescent Olympus AX70 microscope (Omnilabo, Antwerp, Belgium) equipped with a MegaView2 digital camera and analysis software (Soft Imaging System, Munster, Germany), as detailed previously [16,33,35].

Reverse Transcription–Polymerase Chain Reaction

The procedure used for the standard RT-PCR was identical to that described previously [33,35]. The following primers were used: *BEX2* forward 5′-gtgatcggccaacact-3′ and reverse 5′-tccaagcctatgcattatgtc-3′, *BEX1* forward 5′-tagatgggaatatgatgcatagg-3′ and reverse 5′-caggtaaaggtttacaacaagg-3′, actin forward 5′-ctaagtcatagtccgcctag-3′ and reverse 5′-aaatcgtgcgtgacattaagg-3′, and Gal-1 forward 5′-agcaacctgaatctcaaacc-3′ and reverse 5′-cttgaattcgtatccatctgg-3′. The PCR conditions for all primer pairs, except actin, were predenaturation: 4 minutes, 94°C, PCR amplification: 35 cycles at 94°C, 30 seconds (denaturation), 59°C, 30 seconds (annealing), 72°C, 1 minute (extension); and final extension: 1 cycle at 72°C, 10 minutes. For actin, the PCR conditions were predenaturation: 4 minutes, 94°C, PCR amplification: 25 cycles at 94°C, 30 seconds (denaturation), 62°C, 30 seconds (annealing), 72°C, 1 minute (extension); and final extension: 1 cycle at 72°C, 10 minutes.

Statistical Analyses

Survival analyses were carried out by means of Kaplan-Meier curves, which were compared with the log-rank test. Statistical comparisons between control and treated groups were established by carrying out the Kruskal-Wallis test (a nonparametric one-way analysis of variance). When this multigroup test was significant, *post hoc* tests (Dunn procedure) were used to compare the group pairs of interest, thus avoiding multiple comparison effects. Data correlation was analyzed by means of the nonparametric Spearman correlation index and its associated statistical test. All the statistical analyses were realized using Statistica (Statsoft, Tulsa, OK).

Results

BEX1 and BEX2 Expression in Human Malignant Gliomas and Human Normal Brain Tissues

We first analyzed the genomic expression of *BEX2* and its closely related family member *BEX1* in a series of glioma and normal brain tissue samples, and we observed that *BEX1* genomic expression appreciably correlated to *BEX2* genomic expression in gliomas ($r = 0.71$; $P < .001$ Spearman test; Figure 1A). However, the patterns of *BEX1* and *BEX2* expression differed as illustrated in Figure 1, B and C. Indeed, whereas *BEX1* expression gradually decreased according to the sequence normal > oligodendrogliomas > astrocytomas > highly malignant astrogliomas (Figure 1B), *BEX2* expression was globally lower in all glioma groups when compared with normal brain tissues (Figure 1C), with the exception that expression in the oligodendroglioma grade 2 group was higher than that in glioblastomas (Figure 1C).
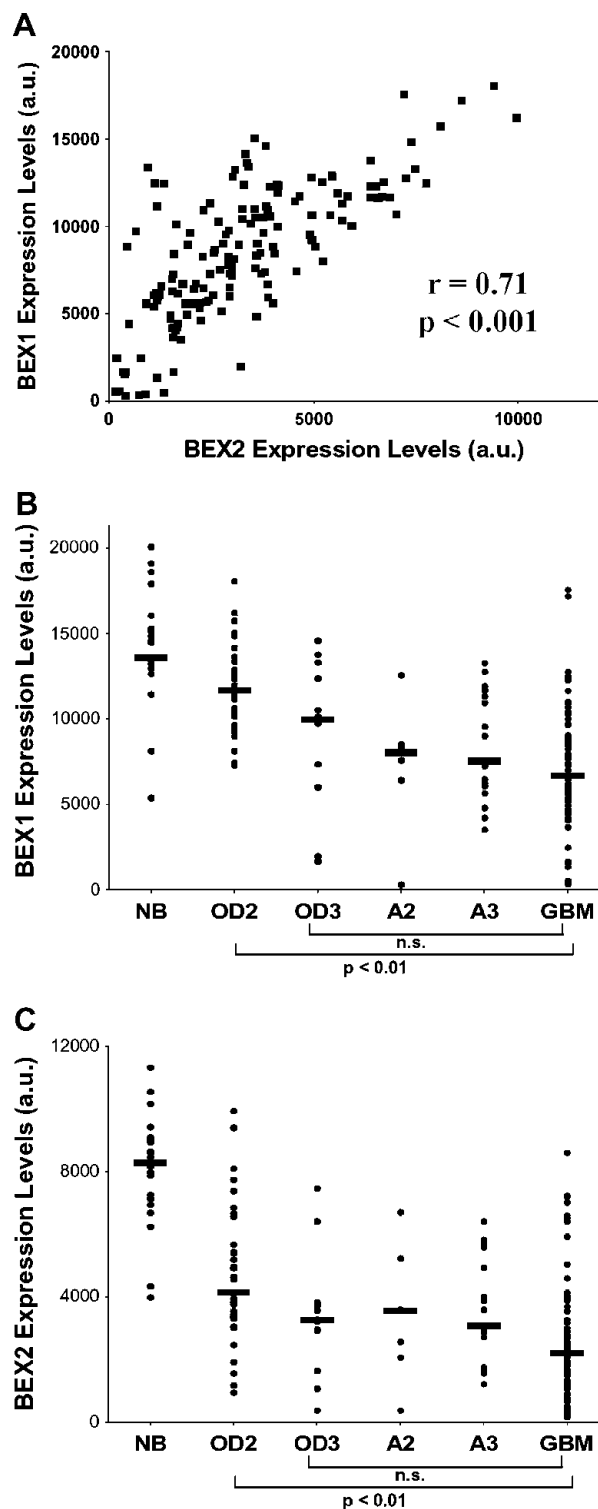

Figure 1. (A) Comparison of *BEX1 versus BEX2* genomic expression in a series of 153 human glioma samples (see A and B). *BEX1* (B) and *BEX2* (C) genomic expression analyzed in 23 normal brain tissue samples (NB), 7 grade 2 astrocytomas (A2), 19 grade 3 astrocytomas (A3), 77 GBMs, 38 grade 2 oligodendrogliomas (OD2), and 12 grade 3 oligodendrogliomas (OD3). Each case is symbolized by a black dot, and the bars represent median values.

Decreasing Gal-1 Expression in Hs683 Oligodendroglioma Cells Induces a Decrease in BEX2 Expression

BEX1 and *BEX2* are 85% identical [18], and therefore, to ensure that we pursued our studies solely on *BEX2*, *BEX1 versus BEX2* expression was analyzed (by means of an RT-PCR technique) in four human permanent cell lines from the ATCC (including the Hs683 oligodendroglioma model) and in four astroglioma primocultures. Figure 2*A* shows that the oligodendroglioma Hs683 cell line and the U373 and T98G astroglioma cell lines do not express *BEX1*. When performing genome-wide analysis of Hs683 cells transiently transfected with siRNA targeting Gal-1 [15,16], it was observed that *BEX2* was the gene whose expression was the most modified of a series of approximately 140 genes. Indeed, the levels of *BEX2* mRNA were decreased by >20-fold in anti–Gal-1–transfected Hs683 cells compared with wt or CT siRNA-transfected cells as revealed in the whole-genome Affymetrix analysis or here by means of PCR analysis (Figure 2*B*). The decrease of *BEX2* expression in anti–Gal-1–transfected cells was also confirmed by means of quantitative RT-PCR (data not shown).

Confirmation That the siRNA Approach Decreases BEX2 Expression in Hs683 Cells

Figure 2*C* shows that the anti-*BEX2* siRNA we designed successfully decreased *BEX2* mRNA levels in Hs683 oligodendroglioma cells up to days 5 and 6 after transfection, whereas the levels of Gal-1 mRNA remained unchanged. The levels of BEX2 protein (quantitatively determined by means of computer-assisted fluorescence microscopy) were also significantly decreased up to day 7 after transfection (Figure 2*D*). Additional experiments showed that the decrease in *BEX2* mRNA levels in Hs683 cells lasted for 8 to 9 days (data not shown).

Decreasing BEX2 Expression in Hs683 Cells Increases the Survival of Hs683 Orthotopic Xenograft-Bearing Mice

Immunocompromised mice grafted with Hs683 oligodendroglioma cells transfected with anti-*BEX2* siRNA revealed a significant (*P* < .05) but modest increase in survival (*blue circles*) compared with mice grafted with wt (*black circles*) or CT siRNA-transfected Hs683 cells
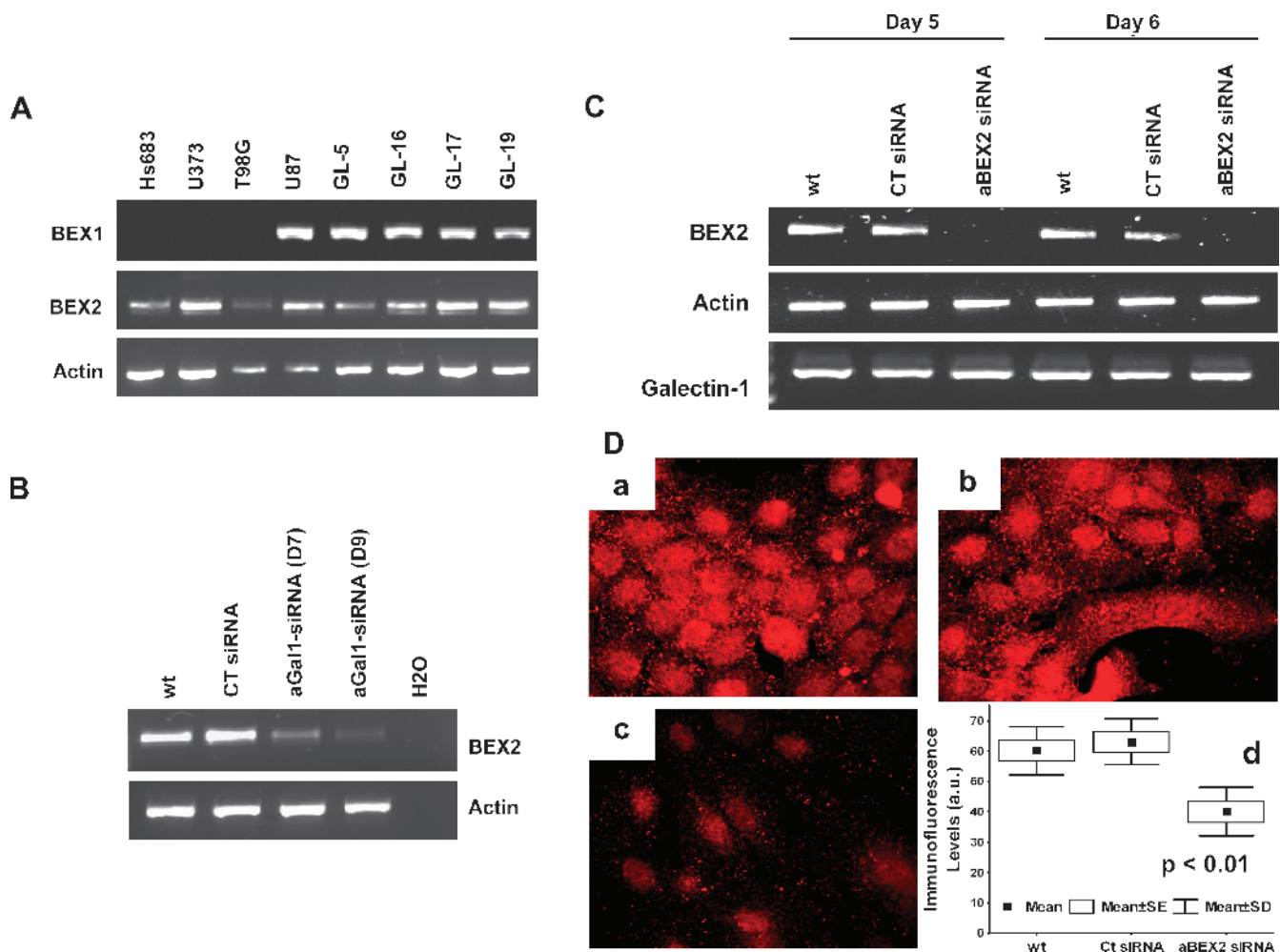

Figure 2. (A) Expression of *BEX1* and *BEX2* mRNA in eight different human glioma cell lines (four established cell lines, namely, Hs683, U373, T98G, and U87, and four primocultures, namely, GL-5, GL-16, GL-17, and GL-19) assessed by RT-PCR. (B) Expression of *BEX2* mRNA in human Hs683 cells: wild-type non-transfected (wt), CT siRNA-transfected (CT siRNA), or anti–Gal-1 siRNA-transfected (aGal-1–siRNA) on days 7 and 9 after transfection, assessed by RT-PCR. (C) Expression of *BEX2* mRNA in Hs683 cells: wild-type nontransfected (wt), CT siRNA-transfected (CT siRNA), or anti-*BEX2* siRNA-transfected (aBEX2 siRNA) on days 5 and 6 after transfection, assessed by RT-PCR. (D) Immunofluorescence analysis of *BEX2* expression in Hs683 cells on day 7 after transfection in wild-type nontransfected (Da) or CT siRNA-transfected (Db) or anti-BEX2 siRNA-transfected (Dc). (Dd) *BEX2* expression quantitatively determined by means of computer-assisted fluorescence microscopy in wild type (wt) and transfected Hs683 cells.

(*red circles*; Figure 3*A*). This experiment has been conducted twice with similar results (data for the second experiment are not shown).

BEX2 *Is Implicated in Hs683 Oligodendroglioma Neoangiogenesis In Vivo*

As Gal-1 has been shown to play an important role in angiogenesis, we investigated whether decreasing *BEX2* expression in Hs683 oligodendroglioma orthotopic xenografts in immunocompromised mice (Figure 3*Ba*) impaired neoangiogenesis features. For this purpose, 11 mice per group orthotopically grafted with wt, control, or anti-*BEX2* siRNA–transfected Hs683 cells underwent euthanasia on day 17 after tumor grafting. The blood vessels in the tumor were stained by immunohistochemistry using an anti-CD34 antibody. The typical blood vessels taken into account to assess angiogenesis
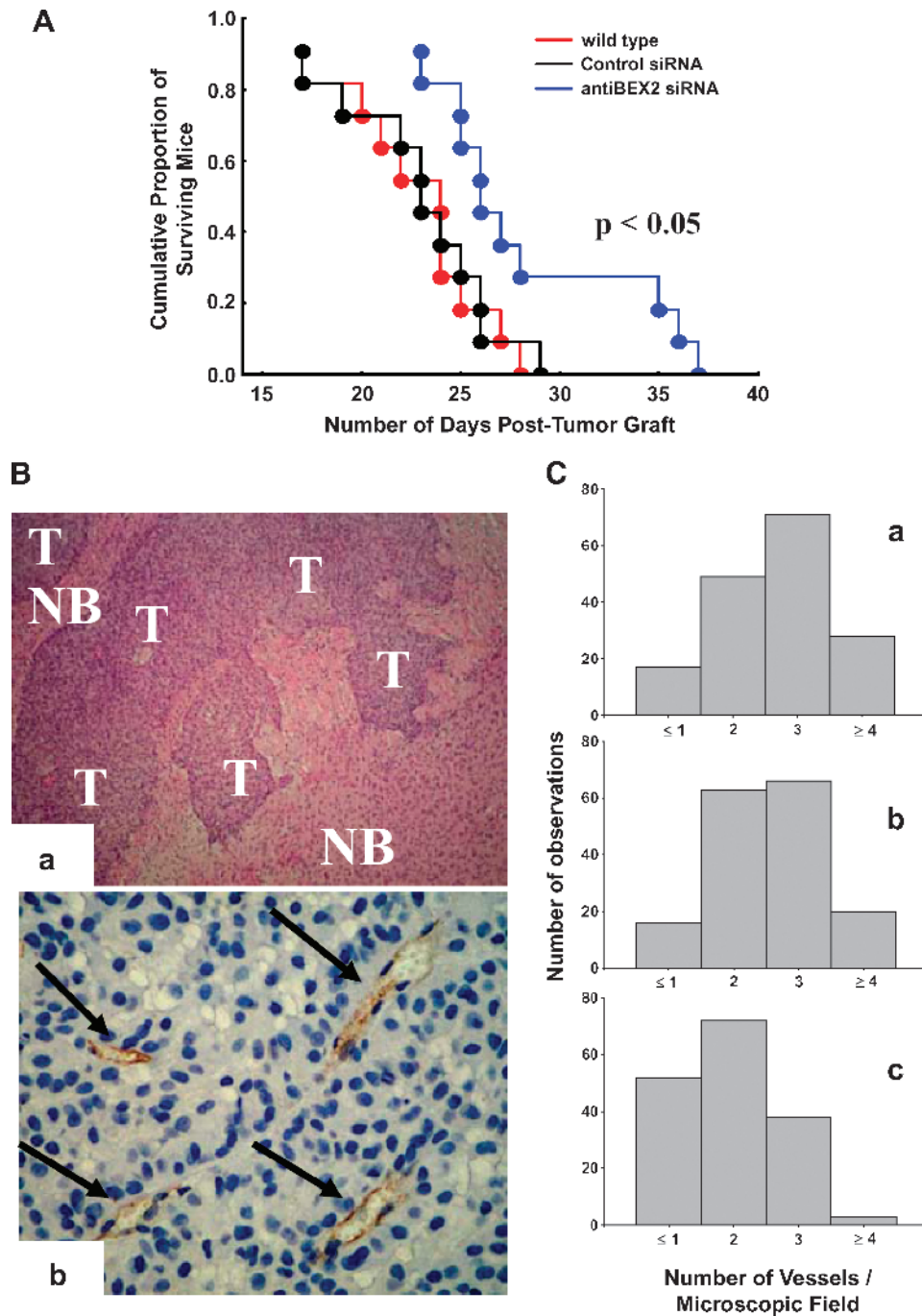

Figure 3. (A) Survival of immunocompromised mice with brain xenografts of wild-type nontransfected human Hs683 cells (red circles), Hs683 cells transfected *in vitro* with CT siRNA (black circles), or anti-BEX2 siRNA (blue circles). (Ba) Morphological illustration of the invasive patterns of Hs683 after orthotopic xenografts into the brains of immunocompromised mice (hematoxylin and eosin–stained; magnification, ×10). *NB* indicates normal brain tissue; *T*, tumor. (Bb) Illustration of the blood vessels (black arrows) stained with an anti-CD34 antibody in Hs683 xenografts (magnification, ×40). In this picture (wt condition), we can observe four blood vessels on one microscopic field. (C) Distribution of the blood vessel counts on 165 microscopic fields in wild type (wt: Ca), CT siRNA- (Cb), or anti-BEX2 siRNA- (Cc) transfected Hs683 orthotopic xenografts.
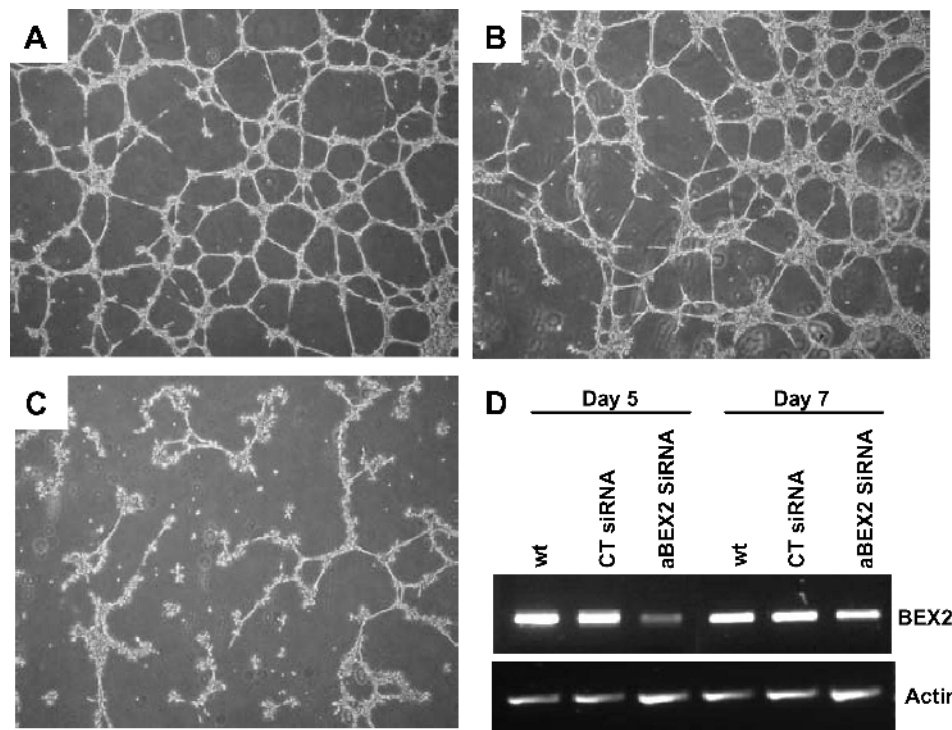
Figure 4. Wild-type (A) and CT siRNA-transfected (B) Hs683 cells developed vasculogenic capillary networks when cultured on Matrigel, whereas Hs683 cells (C) transfected with anti-BEX2 siRNA did not. (D) Confirmation of decrease in *BEX2* mRNA in anti-*BEX2* siRNA-transfected (aBEX2 siRNA) compared with wild-type nontransfected (wt) and CT siRNA-transfected (CT siRNA) Hs683 cells on days 5 and 7 after transfection, assessed by RT-PCR.

in Hs683 tumors are illustrated in Figure 3*Bb*. Decreasing *BEX2* expression in Hs683 xenografts significantly ($P < .01$) decreased the number of blood vessels within these tumors (Figure 3*Cc*) compared with controls (Figure 3, *Ca* and *Cb*).

Ability to Elicit Vasculogenic Mimicry Differs in Wild-type, CT siRNA-, and Anti-BEX2 siRNA-Transfected Hs683 Cells In Vitro

Gross histological examination as performed and illustrated in Figure 3*B* cannot distinguish between true angiogenesis and vasculogenic mimicry processes. Aggressive tumors, including, for example, melanomas, may generate tumor cells that form vascular channels that facilitate perfusion independent of tumor angiogenesis [37]. Vasculogenic mimicry has also been shown to be a feature of gliomas [38]. In addition, we have reported previously that Gal-1 is implicated *in vitro* in vasculogenic mimicry performed by Hs683 oligodendroglioma cells [16]. Accordingly, differences in the patterns of vasculogenic mimicry between wt, CT siRNA-, and anti-*BEX2* siRNA-transfected Hs683 cells were investigated. The data reveal that when wt (Figure 4*A*) and control-transfected (Figure 4*B*) Hs683 cells were cultured on Matrigel, networking processes resembling vasculogenic mimicry were observed. In contrast, anti-*BEX2* siRNA-transfected Hs683 cells no longer demonstrated these vasculogenic processes (Figure 4*C*). Figure 4*D* confirms that the siRNA against *BEX2* actually decreased its expression compared with wt and CT siRNA-transfected Hs683 cells, although this decrease of *BEX2* expression was not as strong as what was obtained with the previous transfection (Figure 2*C*).

Decreasing BEX2 Expression in Hs683 Cells Impairs Their Migration Characteristics

Reducing *BEX2* expression in Hs683 cells seemed to have no impact on anchorage-dependent or -independent growth, cell cycle kinetics or proliferation rate, cell motility when cultured on plastic or Matrigel, susceptibility to apoptosis, or increased sensitivity to two cytotoxic drugs investigated (TMZ and carmustine). These data are summarized for the sake of clarity in Table 1.

However, striking effects relating to cell migration including adhesion and invasion were observed when decreasing *BEX2* expression. Indeed, decreasing *BEX2* expression significantly ($P < .001$) increased the levels of adhesion of Hs683 cells cultured in Matrigel or in fibronectin (Figure 5*A*). In addition, although quantitative videomicroscopy revealed that impairing *BEX2* expression did not modify Hs683 two-dimensional cell motility when cultured on plastic or Matrigel (Table 1), decreasing BEX2 expression significantly impaired their ability to invade (three-dimensional) Matrigel-coated membranes in Boyden chamber assays (Figure 5*B*).

Decreasing BEX2 Expression in Hs683 Cells Modifies the mRNA Levels of Several Genes Implicated in Cell Migration

Previous studies and present data show that 1) Gal-1 exerts potent promigratory effects [10–12], 2) impairing Gal-1 expression reduces *BEX2* expression (Figure 2*B*), and 3) *BEX2* seems to be implicated in migration (Figure 5). For these reasons, we carried out microarray analysis to compare gene expression in wt, anti-*BEX2* siRNA-transfected, and control siRNA-transfected Hs683 cells. Of the 26 genes whose expression was significantly upregulated or downregulated (i.e., ≥1.6- or ≤0.6-fold, respectively) 8 are known to exert a role in cell migration

Table 1. Summary of Experiments Undertaken to Investigate BEX2-Mediated Biological Effects in Human Hs683 GBM Cells.

Cell Biology Feature Evaluated	Techniques Used	References Fully Detailing Technique Used	Comments to Data Obtained in the Current Study
Cell population kinetics			
Anchorage-dependent global cell growth	MTT colorimetric assay	[39,40]	Decreasing *BEX2* expression in Hs683 cells did not modify their anchorage-dependent growth.
Anchorage-independent cell growth	Soft-agar clonogenic assay	[34]	Decreasing *BEX2* expression in Hs683 cells did not modify their anchorage-independent growth.
Cell proliferation (cell cycle kinetics)	Flow cytometry analysis of propidium iodide–stained cells	[32]	Decreasing *BEX2* expression in Hs683 cells did not modify cell cycle kinetics or their proliferation rate.
Cell death (apoptosis)	Flow cytometry analysis of TUNNEL-propidium iodide–stained cells	[32]	Decreasing *BEX2* expression in Hs683 cells did not induce apoptosis.
Cell migration			
Motility	Computer-assisted phase-contrast microscopy (quantitative videomicroscopy)	[10,11,35]	Decreasing *BEX2* expression in Hs683 cells did not modify their motility levels when cultured on plastic or Matrigel.
Sensitivity to anticancer drugs			
Anchorage-dependent cell growth	MTT colorimetric assay	[15]	Decreasing *BEX2* expression in Hs683 cells did not modify their sensitivity to the cytotoxic effects of TMZ or *BCNU*.

(*MAP2, ITGB6, VIL1, MMP7, PLXNC1, CCL2, NT5E*, and *SWAP70*; Table 2).

Figure 6 illustrates the data obtained at the protein level with respect to four of the eight genes listed in Table 2: microtubule-associated protein 2 (*MAP2*), *plexin C1*, switch-associated protein 70 (*SWAP70*), and *integrin β_6*. Transiently decreasing BEX2 expression in Hs683 cells markedly increased MAP2 expression, slightly increased plexin C1 expression, and abolished SWAP70 expression (Figure 6A). Decreasing BEX2 expression also markedly increased integrin β_6 expression (Figure 6B). Moreover, IF analysis revealed a diffuse staining pattern for integrin β_6 in Hs683 cells transfected with control CT siRNA (Figure 6, *Ca* and *Cb*), whereas marked integrin β_6 clustering at the level of lamelipodia became apparent when decreasing *BEX2* expression (Figure 6, *Cc* and *Cd*).

Moreover, transiently decreasing Gal-1 expression in Hs683 cells also increased MAP2 and plexin C1 (Figure 6A). These data strongly suggest that *BEX2* could exert its modulatory influences on MAP2 and plexin C1 expression under Gal-1 control, whereas it could exert such an influence on integrin β_6 and SWAP70 without Gal-1 control (Figure 6A).

Discussion

Galectin 1 has been shown to be a key player in astroglioma and oligodendroglioma cell migration [10–12] and oligodendroglioma neoangiogenesis [16] and chemoresistance [15]. In a previous study, we observed that the gene whose expression is the most decreased in response to siRNA-targeted against Gal-1 in Hs683 oligodendroglioma cells is *BEX2* [16]. It would also be interesting to analyze the levels of expression of *BEX2* in oligodendroglioma cell types that are not expressing Gal-1 and to investigate whether exogenous addition of Gal-1 will stimulate *BEX2* expression. However, we could not find any oligodendroglioma (and even astroglioma) cell lines that do not express Gal-1.

In this study, *BEX2* expression has been found to be lower in glioblastomas than in normal brain tissues and low-grade oligodendrogliomas (Figure 1). This could relate to the fact that epigenetic processes may silence *BEX2* expression in glioblastomas [21]. When Foltz et al. [21] treated astroglioma cells with trichostatin A, a histone deacetylase inhibitor or with 5-aza-2′-deoxycytidine, a DNA methyltransferase inhibitor, to identify epigenetically silenced genes, they
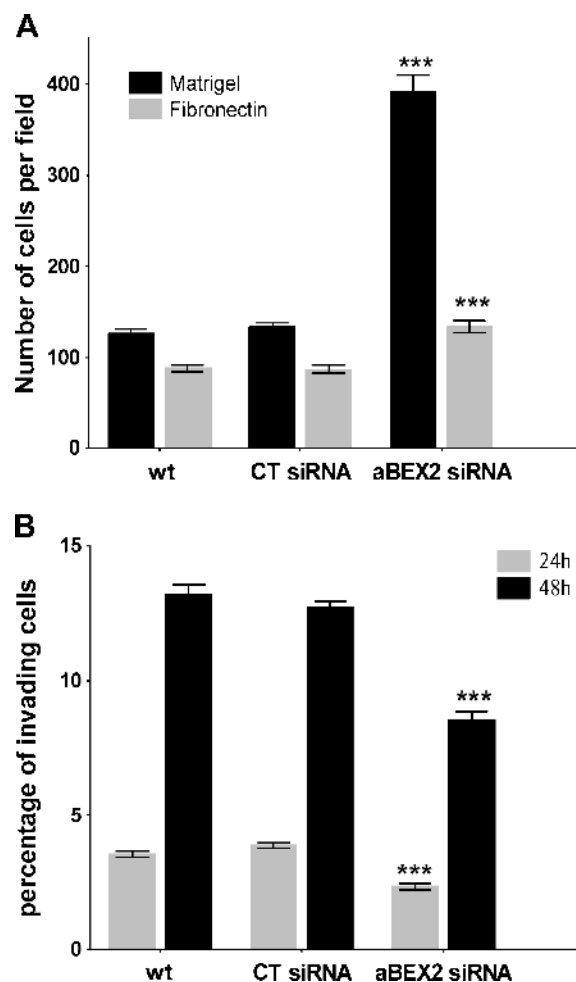
Figure 5. (A) Characterization of the adhesive properties of wild type (wt), control siRNA- (CT siRNA), or anti-*BEX2* siRNA-transfected (aBEX2 siRNA) Hs683 cells on fibronectin (gray bars) or on Matrigel (black bars) supports. Values are the mean ± SEM; ***$P < .001$ compared with CT siRNA. (B) Characterization of Hs683 cell invasiveness in Boyden chambers coated with Matrigel of wild type (wt), CT siRNA-, or anti-BEX2 siRNA-transfected cells after 24 (gray bars) or 48 hours (black bars). Values are the mean ± SEM; ***$P < .001$ compared with CT siRNA.

Table 2. Migration-Related Genes Whose mRNA Expression Was Modified in Hs683 GBM Cells with Reduced *BEX2* Expression.

Official Gene Symbol	Gene Name	Ratio 1: wt/aBEX2 siRNA	Ratio 2: CT siRNA/aBEX2 siRNA	References to Cell Migration
MAP2	Microtubule-associated protein 2	0.4	0.5	[41,42]
ITGB6	Integrin beta 6	0.4	0.5	[43,44]
VIL1	Villin 1	0.4	0.5	[45,46]
MMP7	Matrix metalloproteinase 7 (matrilysin, uterine)	0.6	0.5	[47]
PLXNC1	Plexin C1	0.3	0.6	[48]
CCL2	Chemokine (C-C motif) ligand 2	0.6	0.6	[49–51]
NT5E	5′-Nucleotidase, ecto (CD73)	1.6	1.7	[52,53]
SWAP70	SWAP-70 protein	1.6	2.1	[54,55]

Ratios of gene expression in 1) wild type (wt)/anti-*BEX2* siRNA-transfected Hs683 cells and 2) CT siRNA/anti-*BEX2* siRNA-transfected Hs683 cells.

identified *BEX1* and *BEX2* to be silenced in all tumor specimens because of extensive promoter hypermethylation. Viral-mediated re-expression of either *BEX1* or *BEX2* led to increased sensitivity to chemotherapy-induced apoptosis and showed potent tumor suppressor effects *in vitro* and in a xenograft mouse model *in vivo* [21]. In sharp contrast to the data reported by Foltz et al., Naderi et al. [22] could not detect any correlation in their series of breast cancers between *BEX2* methylation and expression. The *BEX2* promoter is not methylated in Hs683 oligodendroglioma cells (data not shown). Naderi et al. [22] also showed that *BEX2* was overexpressed in a subset of primary breast cancers and that this expression was necessary for the antiapoptotic function of the nerve growth factor in C2-treated cells. These authors suggest that the nerve growth factor/BEX2/nuclear factor-κβ pathway could be involved in regulating apoptosis in breast cancer cells and in modulating the response to tamoxifen in primary breast cancers [22]. In the current study, decreasing *BEX2* expression in Hs683 oligodendroglioma cells did not increase their sensitivity to TMZ or carmustine or lead to modifications in cell proliferation, cell death (apoptosis), or anchorage-dependent or -independent growth (Table 1). In addition, in contrast to the study of Foltz et al. [21], which relied on the analysis of astroglial cells, transiently decreasing *BEX2* expression in Hs683 oligodendroglioma cells induced modest but nevertheless significant increases in the survival of Hs683 orthotopic xenograft-bearing mice. It thus seems that *BEX2* biological functions and activity could markedly differ between astroglioma and oligodendroglioma cells, a feature which we already emphasized in the introduction with respect to the gene products *PDGF* [5], *EGFR* [7], *vimentin* [25], *integrin β_4* [24], *ATAD 3B* [26], and *Notch2* [27].
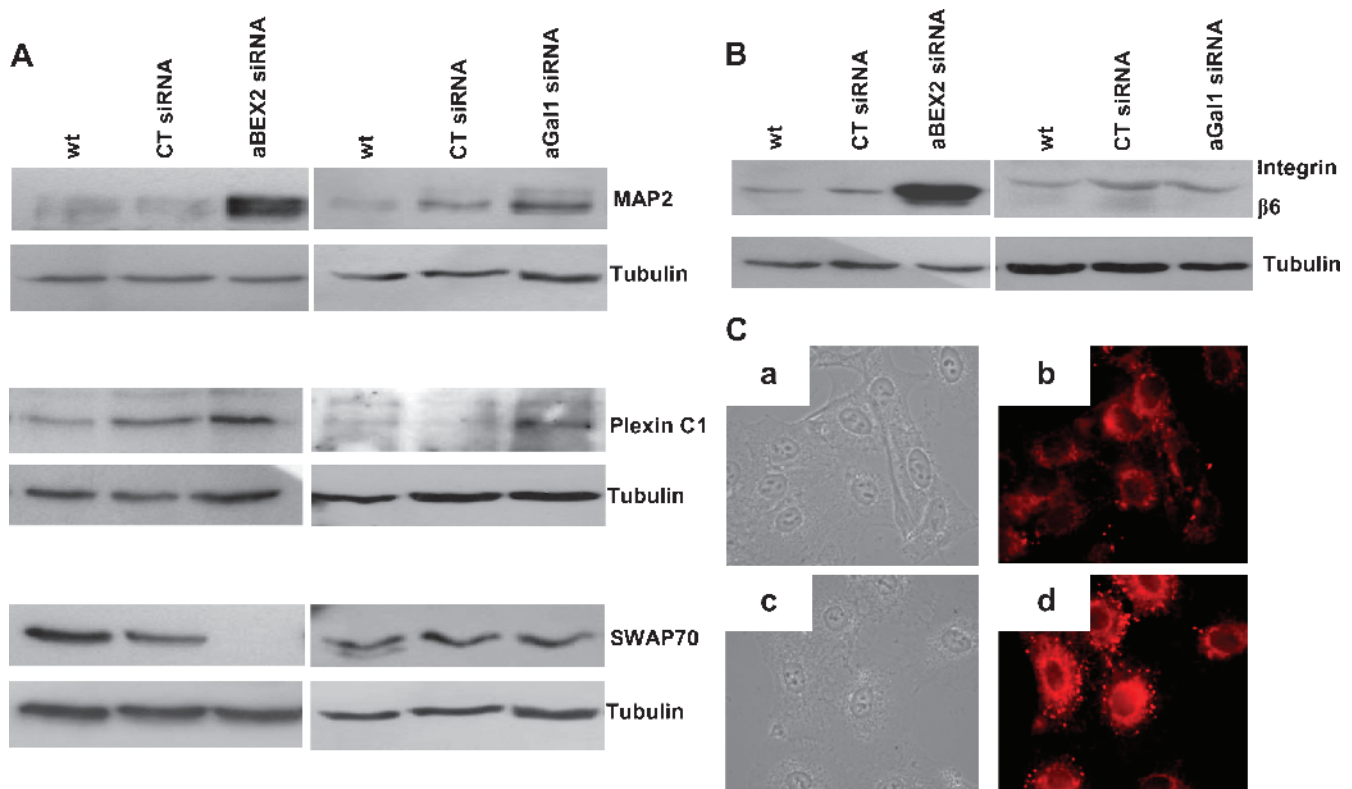

Figure 6. (A) Western blot analysis of *MAP2*, *plexin C1*, and *SWAP70* expression in wild type (wt), CT siRNA-transfected (CT siRNA), anti-*BEX2* siRNA-transfected (aBEX2 siRNA), and anti–Gal-1 siRNA-transfected (aGal-1 siRNA) Hs683 cells on day 5 after transfection. (B) Western blot analysis of *integrin β_6* expression in wt, CT siRNA, aBEX2 siRNA-transfected, and aGal-1 siRNA-transfected Hs683 cells on day 5 after transfection. (C) Immunofluorescence analysis (with bright field controls) of *integrin β_6* expression in CT siRNA- (Ca and Cb) and aBEX2 siRNA-transfected (Cc and Cd) Hs683 cells on day 5 after transfection.

Decreasing *BEX2* expression in Hs683 oligodendroglioma cells impairs angiogenesis in Hs683 xenografts when these cells are orthotopically grafted *in vivo* into the brains of immunocompromised mice (Figure 3). It is worthwhile to note that the type of staining we performed with CD34 does not allow for differentiation between tumor neoangiogenesis and normal vessels trapped within tumor tissues. The use of antibodies directed against specific markers of tumor endothelial cells, such as CD105 [56] or Dkk-3 [57], would be useful to determine if *BEX2* is indeed involved in tumor neoangiogenesis. However, although these markers have been proven effective to determine neoangiogenesis through immunohistochemistry in human tissue [56,57], we failed to be able to use these markers in the present study to make this determination in mouse tissue (data not shown).

A previous study [16] and the current one revealed that *BEX2* expression is controlled, at least partly, by Gal-1. Galectin 1 has been shown to exert its proangiogenic effects, at least partly, through the endoplasmic reticulum transmembrane kinase/ribonuclease IRE-1α–mediated control of the expression of oxygen-related protein 150, which, in turn, controls VEGF expression [16]. Once more, the patterns of VEGF expression [58] and vasculature profiles [59] differ between astrogliomas and oligodendrogliomas. Transiently decreasing *BEX2* expression in Hs683 cells did not modify VEGF expression and decreasing IRE-1α expression in these Hs683 cells did not modify *BEX2* expression (data not shown). This suggests that Gal-1–mediated control of *BEX2* is independent of the activation of IRE-1α and that the *BEX2*-related effects on angiogenesis and on vasculogenic mimicry are therefore IRE-1α–independent. The signaling pathway by which *BEX2* exerts its effects on angiogenesis remains to be elucidated.

Decreasing *BEX2* expression in Hs683 oligodendroglioma cells markedly impacts cell migration features *in vitro* on Matrigel or on fibronectin supports with respect to both cell adhesion and cell invasion (Figure 5). Maniotis et al. [60] suggested that formation of vasculogenic mimicry channels is related to the invasive ability of tumor cells. The fact that decreasing *BEX2* expression impairs the invasive properties of Hs683 glioma cells (Figure 5*B*) might then partly explain the effects observed on vasculogenic mimicry *in vitro* (Figure 4) and angiogenesis *in vivo* (Figure 3). The effects observed on cell adhesion and invasion could be partly explained by the fact that decreasing *BEX2* expression induces the up or down-regulation of a number of genes involved in migration (Table 2) including notably *MAP2*, *plexin C1*, *integrin* β_6, and *SWAP70*.

MAP2, a member of the microtubule-associated proteins that can bind both microtubules and F-actin [61], has been shown to play a role in cell migration [41,42]. Interestingly, we have shown previously that the knockdown of Gal-1 expression in U87 astroglioma cells also decreased their motility and induced an increase in *MAP2* expression [12].

Plexin C1 is a member of the plexin family of semaphorin receptors. Semaphorin binding to plexin receptors can regulate actin cytoskeleton rearrangement through the regulation of the activity of small GTPases of the Rho and Rac families [62]. Galectin 1 controls, at least partly, glioma cell migration through RhoA-mediated modifications of the actin cytoskeleton [11]. Semaphorins have also been shown to regulate adhesive and migratory properties of malignant cells [63], at least through modulation of integrin-mediated adhesion and migration [48]. Decreasing *BEX2* in Hs683 oligodendroglioma cells induces a marked increase in *integrin* β_6 expression (Figure 6*B*) and its clustering in lamelipodia (Figure 6*C*). The expression of *integrin* β_6 has been shown to increase migration and the invasive behavior of oral squamous cell carcinomas [43]. Our observation that the localization of *integrin* β_6 changed toward clustering in lamelipodia (Figure 6*C*) when *BEX2* expression decreases could possibly explain the resulting phenotype of increased adhesion (Figure 5*A*) and reduced invasion (Figure 5*B*). We recently showed that depletion of Gal-1 through both stable knockdown and transient-targeted siRNA treatment against Gal-1 induces an intracellular accumulation of *integrin* β_1 coincident with a diminution of *integrin* β_1 at points of cellular adhesion at the cell membrane in Hs683 oligodendroglioma and U87 astroglioma cells [64]. Galectin 1 depletion does not alter the gene expression level of *integrin* β_1 but effectuates the perinuclear accumulation of protein kinase C epsilon and the intermediate filament vimentin, both of which have been shown to mediate integrin recycling in motile cells [64].

Finally, it was observed that transiently decreasing *BEX2* expression in Hs683 cells strongly reduced the expression of *SWAP70* (Figure 6), a form of Rac-GEF that transduces signals from tyrosine kinase receptors to Rac [65]. *SWAP70* has been shown to be associated with a subset of actin filaments generated in lamelipodia and the membrane ruffles of motile cells [54]. Moreover, *SWAP70* has also been shown to modulate cell adhesion to fibronectin, homotopic cell aggregation, and migration [55].

Moreover, we have shown that the decrease of Gal-1 expression also impairs the expression of *MAP2* and *plexin C1*. These results tend to confirm that Gal-1 could control the expression of *BEX2*, which, in turn, modulates the expression of genes involved in cell migration.

In conclusion, the present study has revealed Gal-1–mediated control of *BEX2* expression and the involvement of *BEX2* in oligodendroglioma neoangiogenesis and oligodendroglioma cell migration. It is also suggested that these effects may be partly explained by modulation of the expression of a number of genes such as *MAP2*, *plexin C1*, *integrin* β_6, and *SWAP70* that have already been shown to play a role in cancer cell migration.

References

[1] Louis DN (2006). Molecular pathology of malignant gliomas. *Annu Rev Pathol* **1**, 97–117.

[2] Lefranc F, Brotchi J, and Kiss R (2005). Possible future issues in the treatment of glioblastomas: special emphasis on cell migration and the resistance of migrating glioblastoma cells to apoptosis. *J Clin Oncol* **23**, 2411–2422.

[3] Lefranc F, Facchini V, and Kiss R (2007). Proautophagic drugs: a novel means to combat apoptosis-resistant cancers, with a special emphasis on glioblastomas. *Oncologist* **12**, 1395–1403.

[4] Van den Bent MJ, Reni M, Gatta G, and Vecht C (2008). Oligodendroglioma. *Crit Rev Oncol Hematol* **66**, 262–272.

[5] Dai C, Lyustikman Y, Shih A, Hu X, Fuller GN, Rosenblum M, and Holland EC (2005). The characteristics of astrocytomas and oligodendrogliomas are caused by two distinct and interchangeable signaling formats. *Neoplasia* **7**, 397–406.

[6] Hu X, Pandolfi PP, Li Y, Koutcher JA, Rosenblum M, and Holland EC (2005). mTOR promotes survival and astrocytic characteristics induced by Pten/AKT signaling in glioblastoma. *Neoplasia* **7**, 356–368.

[7] Ducray F, Idbaih A, de Reynies A, Bieche I, Thillet J, Mokhtari K, Lair S, Marie Y, Paris S, Vidaud M, et al. (2008). Anaplastic oligodendrogliomas with 1p19q codeletion have a proneural gene expression profile. *Mol Cancer* **7**, 41.

[8] Liu FT and Rabinovich GA (2005). Galectins as modulators of tumour progression. *Nat Rev Cancer* **5**, 29–41.

[9] Camby I, Le Mercier M, Lefranc F, and Kiss R (2006). Galectin 1: a small protein with major functions. *Glycobiology* **16**, 137R–157R.

[10] Camby I, Belot N, Rorive S, Lefranc F, Maurage CA, Lahm H, Kaltner H, Hadari Y, Ruchoux MM, Brotchi J, et al. (2001). Galectins are differentially expressed in supratentorial pilocytic astrocytomas, astrocytomas, anaplastic as-

trocytomas and glioblastomas, and significantly modulate tumor astrocyte migration. *Brain Pathol* **11**, 12–26.

[11] Camby I, Belot N, Lefranc F, Sadeghi N, de Launoit Y, Kaltner H, Musette S, Darro F, Danguy A, Salmon I, et al. (2002). Galectin 1 modulates human glioblastoma cell migration into the brain through modifications to the actin cytoskeleton and levels of expression of small GTPases. *J Neuropathol Exp Neurol* **61**, 585–596.

[12] Camby I, Decaestecker C, Lefranc F, Kaltner H, Gabius HJ, and Kiss R (2005). Galectin 1 knocking down in human U87 glioblastoma cells alters their gene expression pattern. *Biochem Biophys Res Commun* **335**, 27–35.

[13] Le QT, Shi G, Cao H, Nelson DW, Wang Y, Chen EY, Zhao S, Kong C, Richardson D, O'Byrne KJ, et al. (2005). Galectin 1: a link between tumor hypoxia and tumor immune privilege. *J Clin Oncol* **23**, 8932–8941.

[14] Strik HM, Schmidt K, Lingor P, Tonges L, Kugler W, Nitsche M, Rabinovich GA, and Bahr M (2007). Galectin 1 expression in human glioma cells: modulation by ionizing radiation and effects on tumor cell proliferation and migration. *Oncol Rep* **18**, 483–488.

[15] Le Mercier M, Lefranc F, Mijatovic T, Debeir O, Haibe-Kains B, Bontempi G, Decaestecker C, Kiss R, and Mathieu V (2008). Evidence of galectin 1 involvement in glioma chemoresistance. *Toxicol Appl Pharmacol* **229**, 172–183.

[16] Le Mercier M, Mathieu V, Haibe-Kains B, Bontempi G, Mijatovic T, Decaestecker C, Kiss R, and Lefranc F (2008). Knocking down galectin 1 in human hs683 glioblastoma cells impairs both angiogenesis and endoplasmic reticulum stress responses. *J Neuropathol Exp Neurol* **67**, 456–469.

[17] Thijssen VL, Postel R, Brandwijk RJ, Dings RP, Nesmelova I, Satijn S, Verhofstad N, Nakabeppu Y, Baum LG, Bakkers J, et al. (2006). Galectin 1 is essential in tumor angiogenesis and is a target for antiangiogenesis therapy. *Proc Natl Acad Sci USA* **103**, 15975–15980.

[18] Alvarez E, Zhou W, Witta SE, and Freed CR (2005). Characterization of the *Bex* gene family in humans, mice, and rats. *Gene* **357**, 18–28.

[19] Zhang L (2008). Adaptive evolution and frequent gene conversion in the brain expressed X-linked gene family in mammals. *Biochem Genet* **46**, 293–311.

[20] Han C, Liu H, Liu J, Yin K, Xie Y, Shen X, Wang Y, Yuan J, Qiang B, Liu YJ, et al. (2005). Human *Bex2* interacts with LMO2 and regulates the transcriptional activity of a novel DNA-binding complex. *Nucleic Acids Res* **33**, 6555–6565.

[21] Foltz G, Ryu GY, Yoon JG, Nelson T, Fahey J, Frakes A, Lee H, Field L, Zander K, Sibenaller Z, et al. (2006). Genome-wide analysis of epigenetic silencing identifies *BEX1* and *BEX2* as candidate tumor suppressor genes in malignant glioma. *Cancer Res* **66**, 6665–6674.

[22] Naderi A, Teschendorff AE, Beigel J, Cariati M, Ellis IO, Brenton JD, and Caldas C (2007). *BEX2* is overexpressed in a subset of primary breast cancers and mediates nerve growth factor/nuclear factor-kappaB inhibition of apoptosis in breast cancer cell lines. *Cancer Res* **67**, 6725–6736.

[23] Branle F, Lefranc F, Camby I, Jeuken J, Geurts-Moespot A, Sprenger S, Sweep F, Kiss R, and Salmon I (2002). Evaluation of the efficiency of chemotherapy in *in vivo* orthotopic models of human glioma cells with and without 1p19q deletions and in C6 rat orthotopic allografts serving for the evaluation of surgery combined with chemotherapy. *Cancer* **95**, 641–655.

[24] Belot N, Rorive S, Doyen I, Lefranc F, Bruyneel E, Dedecker R, Micik S, Brotchi J, Decaestecker C, Salmon I, et al. (2001). Molecular characterization of cell substratum attachments in human glial tumors relates to prognostic features. *Glia* **36**, 375–390.

[25] Ikota H, Kinjo S, Yokoo H, and Nakazato Y (2006). Systematic immunohistochemical profiling of 378 brain tumors with 37 antibodies using tissue microarray technology. *Acta Neuropathol* **111**, 475–482.

[26] Hubstenberger A, Labourdette G, Baudier J, and Rousseau D (2008). *ATAD 3A* and *ATAD 3B* are distal 1p-located genes differentially expressed in human glioma cell lines and present *in vitro* anti-oncogenic and chemoresistant properties. *Exp Cell Res* **314**, 2870–2883.

[27] Sivasankaran B, Degen M, Ghaffari A, Hegi ME, Hamou MF, Ionescu MC, Zweifel C, Tolnay M, Wasner M, Mergenthaler S, et al. (2009). Tenascin-C is a novel RBPJkappa-induced target gene for Notch signaling in gliomas. *Cancer Res* **69**, 458–465.

[28] Boulay JL, Miserez AR, Zweifel C, Sivasankaran B, Kana V, Ghaffari A, Luyken C, Sabel M, Zerrouqi A, Wasner M, et al. (2007). Loss of NOTCH2 positively predicts survival in subgroups of human glial brain tumors. *PLoS ONE* **2**, e576.

[29] Hu XB, Feng F, Wang YC, Wang L, He F, Dou GR, Liang L, Zhang HW, Liang YM, and Han H (2009). Blockade of Notch signaling in tumor-bearing mice may lead to tumor regression, progression, or metastasis, depending on tumor cell types. *Neoplasia* **11**, 32–38.

[30] Berger W, Spiegl-Kreinecker S, Buchroithner J, Elbling L, Pirker C, Fischer J,

and Micksche M (2001). Overexpression of the human major vault protein in astrocytic brain tumor cells. *Int J Cancer* **94**, 377–382.

[31] Mathieu V, De Neve N, Le Mercier M, Dewelle J, Gaussin JF, Dehoux M, Kiss R, and Lefranc F (2008). Combining bevacizumab with temozolomide increases the antitumor efficacy of temozolomide in a human glioblastoma orthotopic xenograft model. *Neoplasia* **10**, 1383–1392.

[32] Mijatovic T, Mahieu T, Bruyere C, De Neve N, Dewelle J, Simon G, Dehoux MJ, van der Aar E, Haibe-Kains B, Bontempi G, et al. (2008). UNBS5162, a novel naphthalimide that decreases CXCL chemokine expression in experimental prostate cancers. *Neoplasia* **10**, 573–586.

[33] Megalizzi V, Mathieu V, Mijatovic T, Gailly P, Debeir O, De Neve N, Van Damme M, Bontempi G, Haibe-Kains B, Decaestecker C, et al. (2007). 4-IBP, a sigma1 receptor agonist, decreases the migration of human cancer cells, including glioblastoma cells, *in vitro* and sensitizes them *in vitro* and *in vivo* to cytotoxic insults of proapoptotic and proautophagic drugs. *Neoplasia* **9**, 358–369.

[34] Darro F, Cahen P, Vianna A, Decaestecker C, Nogaret JM, Leblond B, Chaboteaux C, Ramos C, Petein M, Budel V, et al. (1998). Growth inhibition of human *in vitro* and mouse *in vitro* and *in vivo* mammary tumor models by retinoids in comparison with tamoxifen and the RU-486 anti-progestagen. *Breast Cancer Res Treat* **51**, 39–55.

[35] Mathieu V, Mijatovic T, van Damme M, and Kiss R (2005). Gastrin exerts pleiotropic effects on human melanoma cell biology. *Neoplasia* **7**, 930–943.

[36] Hwang JH, Smith CA, Salhia B, and Rutka JT (2008). The role of fascin in the migration and invasiveness of malignant glioma cells. *Neoplasia* **10**, 149–159.

[37] Hendrix MJ, Seftor EA, Hess AR, and Seftor RE (2003). Vasculogenic mimicry and tumour-cell plasticity: lessons from melanoma. *Nat Rev Cancer* **3**, 411–421.

[38] Yue WY and Chen ZP (2005). Does vasculogenic mimicry exist in astrocytoma? *J Histochem Cytochem* **53**, 997–1002.

[39] Mijatovic T, Mathieu V, Gaussin JF, De Neve N, Ribaucour F, Van Quaquebeke E, Dumont P, Darro F, and Kiss R (2006). Cardenolide-induced lysosomal membrane permeabilization demonstrates therapeutic benefits in experimental human non–small cell lung cancers. *Neoplasia* **8**, 402–412.

[40] Dumont P, Ingrassia L, Rouzeau S, Ribaucour F, Thomas S, Roland I, Darro F, Lefranc F, and Kiss R (2007). The Amaryllidaceae isocarbostyril narciclasine induces apoptosis by activation of the death receptor and/or mitochondrial pathways in cancer cells but not in normal fibroblasts. *Neoplasia* **9**, 766–776.

[41] Teng J, Takei Y, Harada A, Nakata T, Chen J, and Hirokawa N (2001). Synergistic effects of *MAP2* and *MAP1B* knockout in neuronal migration, dendritic outgrowth, and microtubule organization. *J Cell Biol* **155**, 65–76.

[42] Liu SY, Chen YT, Tseng MY, Hung CC, Chiang WF, Chen HR, Shieh TY, Chen CH, Jou YS, and Chen JY (2008). Involvement of microtubule-associated protein 2 (*MAP2*) in oral cancer cell motility: a novel biological function of *MAP2* in non–neuronal cells. *Biochem Biophys Res Commun* **366**, 520–525.

[43] Koivisto L, Grenman R, Heino J, and Larjava H (2000). Integrins alpha5beta1, alphavbeta1, and alphavbeta6 collaborate in squamous carcinoma cell spreading and migration on fibronectin. *Exp Cell Res* **255**, 10–17.

[44] Ramos DM, But M, Regezi J, Schmidt BL, Atakilit A, Dang D, Ellis D, Jordan R, and Li X (2002). Expression of integrin beta6 enhances invasive behavior in oral squamous cell carcinoma. *Matrix Biol* **21**, 297–307.

[45] Tomar A, Wang Y, Kumar N, George S, Ceacareanu B, Hassid A, Chapman KE, Aryal AM, Waters CM, and Khurana S (2004). Regulation of cell motility by tyrosine phosphorylated villin. *Mol Biol Cell* **15**, 4807–4817.

[46] Lee M, Hadi M, Hallden G, and Aponte GW (2005). Peptide YY and neuropeptide Y induce villin expression, reduce adhesion, and enhance migration in small intestinal cells through the regulation of CD63, matrix metalloproteinase-3, and Cdc42 activity. *J Biol Chem* **280**, 125–136.

[47] Miyata Y, Iwata T, Ohba K, Kanda S, Nishikido M, and Kanetake H (2006). Expression of matrix metalloproteinase-7 on cancer cells and tissue endothelial cells in renal cell carcinoma: prognostic implications and clinical significance for invasion and metastasis. *Clin Cancer Res* **12**, 6998–7003.

[48] Walzer T, Galibert L, Comeau MR, and De Smedt T (2005). Plexin C1 engagement on mouse dendritic cells by viral semaphorin A39R induces actin cytoskeleton rearrangement and inhibits integrin-mediated adhesion and chemokine-induced migration. *J Immunol* **174**, 51–59.

[49] Loberg RD, Day LL, Harwood J, Ying C, St John LN, Giles R, Neeley CK, and Pienta KJ (2006). CCL2 is a potent regulator of prostate cancer cell migration and proliferation. *Neoplasia* **8**, 578–586.

[50] Liu XS, Zhang ZG, Zhang RL, Gregg SR, Wang L, Yier T, and Chopp M (2007). Chemokine ligand 2 (CCL2) induces migration and differentiation of subventricular zone cells after stroke. *J Neurosci Res* **85**, 2120–2125.

[51] Warner KA, Miyazawa M, Cordeiro MM, Love WJ, Pinsky MS, Neiva KG, Spalding AC, and Nor JE (2008). Endothelial cells enhance tumor cell invasion through a crosstalk mediated by CXC chemokine signaling. *Neoplasia* **10**, 131–139.

[52] Zhou P, Zhi X, Zhou T, Chen S, Li X, Wang L, Yin L, Shao Z, and Ou Z (2007). Overexpression of Ecto-5′-nucleotidase (CD73) promotes T-47D human breast cancer cells invasion and adhesion to extracellular matrix. *Cancer Biol Ther* **6**, 426–431.

[53] Wang L, Zhou X, Zhou T, Ma D, Chen S, Zhi X, Yin L, Shao Z, Ou Z, and Zhou P (2008). Ecto-5′-nucleotidase promotes invasion, migration and adhesion of human breast cancer cells. *J Cancer Res Clin Oncol* **134**, 365–372.

[54] Hilpela P, Oberbanscheidt P, Hahne P, Hund M, Kalhammer G, Small JV, and Bahler M (2003). SWAP-70 identifies a transitional subset of actin filaments in motile cells. *Mol Biol Cell* **14**, 3242–3253.

[55] Sivalenka RR and Jessberger R (2004). SWAP-70 regulates c-kit–induced mast cell activation, cell-cell adhesion, and migration. *Mol Cell Biol* **24**, 10277–10288.

[56] Sugita Y, Takase Y, Mori D, Tokunaga O, Nakashima A, and Shigemori M (2007). Endoglin (CD 105) is expressed on endothelial cells in the primary central nervous system lymphomas and correlates with survival. *J Neurooncol* **82**, 249–256.

[57] Untergasser G, Steurer M, Zimmermann M, Hermann M, Kern J, Amberger A, Gastl G, and Gunsilius E (2008). The Dickkopf-homolog 3 is expressed in tumor endothelial cells and supports capillary formation. *Int J Cancer* **122**, 1539–1547.

[58] Huang H, Held-Feindt J, Buhl R, Mehdorn HM, and Mentlein R (2005). Expression of VEGF and its receptors in different brain tumors. *Neurol Res* **27**, 371–377.

[59] Challa VR, Moody DM, Brown WR, and Zagzag D (2004). A morphologic study of the vasculature of malignant gliomas using thick celloidin sections and alkaline phosphatase stain. *Clin Neuropathol* **23**, 167–172.

[60] Maniotis AJ, Folberg R, Hess A, Seftor EA, Gardner LM, Pe'er J, Trent JM, Meltzer PS, and Hendrix MJ (1999). Vascular channel formation by human melanoma cells *in vivo* and *in vitro*: vasculogenic mimicry. *Am J Pathol* **155**, 739–752.

[61] Dehmelt L and Halpain S (2005). The MAP2/Tau family of microtubule-associated proteins. *Genome Biol* **6**, 204.

[62] Castellani V and Rougon G (2002). Control of semaphorin signaling. *Curr Opin Neurobiol* **12**, 532–541.

[63] Neufeld G, Shraga-Heled N, Lange T, Guttmann-Raviv N, Herzog Y, and Kessler O (2005). Semaphorins in cancer. *Front Biosci* **10**, 751–760.

[64] Fortin S, Le Mercier M, Camby I, Spiegl-Kreinecker S, Berger W, Lefranc F, and Kiss R (in press). Galectin 1 is implicated in the protein kinase C epsilon/vimentin–controlled trafficking of integrin-beta1 in glioblastoma cells. *Brain Pathol*.

[65] Shinohara M, Terada Y, Iwamatsu A, Shinohara A, Mochizuki N, Higuchi M, Gotoh Y, Ihara S, Nagata S, Itoh H, et al. (2002). SWAP-70 is a guanine-nucleotide-exchange factor that mediates signalling of membrane ruffling. *Nature* **416**, 759–763.